Research Article

Goshtasp Cheraghian*, Michael P. Wistuba, Sajad Kiani, Ali Behnood, Masoud Afrand, and Andrew R. Barron*

Engineered nanocomposites in asphalt binders

https://doi.org/10.1515/ntrev-2022-0062 received December 1, 2021; accepted January 19, 2022

Abstract: Recently, nanotechnology has been effectively used in the field of road pavement. Oxidation and aging of asphalt cause deterioration of road pavements and increase asphalt-related emissions. We propose an anti-aging strategy to interrupt the asphalt deterioration by using engineered clay/fumed silica nanocomposites. In this research, the morphological, chemical, thermal, mechanical, and rheological properties of nano-modified asphalt binders are meticulously analyzed in various conditions. The experiment results proved that this composite efficiently disrupts the chemical oxidation and decomposition in the mixture and reduces the aging rate. Remarkably, asphalt binder rheology experiments revealed that the addition of 0.2-0.3 wt% of nano-reinforced materials maximized their rheological resistance after shortand long-term aging. Moreover, nanoparticles improve the moisture resistance efficiency and in turn overcome the critical issue of moisture in low production temperature within



e-mail: g.cheraghian@tu-braunschweig.de

Michael P. Wistuba: Braunschweig Pavement Engineering Centre (ISBS), Technische Universität Braunschweig, Braunschweig, Germany

Sajad Kiani: Energy Safety Research Institute (ESRI), Swansea University, Bay Campus, Swansea, SA1 8EN, United Kingdom; College of Engineering, Swansea University Bay Campus, Fabian Way, Swansea, SA1 8EN, United Kingdom

Ali Behnood: Lyles School of Civil Engineering, Purdue University, 550 Stadium Mall, West Lafayette, IN 47907-2051, United States of America

Masoud Afrand: Institute of Research and Development, Duy Tan University, Da Nang 550000, Vietnam



Graphical abstract

the framework of warm mix asphalt technology. This costeffective, facile, and scalable approach in warm mix asphalt mixtures can contribute to increased sustainability and lifespan of pavements and a reduction in greenhouse gas emissions.

Keywords: nano clay, modified bitumen, thermal oxidation aging, nano-modification, nanocomposites

1 Introduction

Bitumen is generally used as the glue in road asphalt mixtures, due to its appropriate rheological properties [1–3]. However, modification of bitumen has developed an emerging field in road material technology, mainly in connection with re-using reclaimed asphalt paving, with low-energy concepts for asphalt mixture production, and with the increasing wish to at least partially replace the bitumen through more sustainable and bio-based binders. A significant issue when identifying the most appropriate bitumen modifiers is to investigate their aging resistance. As road asphalt materials are exposed not only to hot temperatures during mixture production but also to severe sun radiation, and oxygen and other radicals that promote binder aging during their entire in-service life [4-7], the durability of asphalt binders in terms of aging resistance is an important material property. Binder

^{*} Corresponding author: Andrew R. Barron, Energy Safety Research Institute (ESRI), Swansea University, Bay Campus, Swansea, SA1 8EN, United Kingdom; Arizona Institutes for Resilience (AIR), University of Arizona, Tucson, AZ 85721, United States of America; Department of Chemistry, Department of Materials Science and Nanoengineering, Rice University, Houston, Texas 77005, United States of America; Faculty of Engineering, Universiti Teknologi Brunei, Bandar Seri Begawan, Brunei Darussalam, e-mail: a.r.barron@swansea.ac.uk

aging includes ultraviolet, thermal long-term aging, and thermo oxidative short-term aging.

To influence asphalt binder performance, a huge variety of different types of additives can be added to bitumen, such as polymers, fibers, recycled materials, and nanomaterials [8,9]. This study focuses on nanomaterials. Among these materials, usually, nanomaterials significantly change chemical binder properties and in consequence mechanical rheological performance properties. Among the most important parameters describing nanoparticles (NPs), which cause physical properties of nanocomposites unique and different from conventional materials, are their ratio of surface area to volume, shape, chemical composition, and their capability to increase interactions at phase interfaces [10,11]. Metal oxide, inorganic, nanofibers, and nanocomposites are the main class of nanomaterials particularly used in asphalt mixture to modify asphaltene binders [12,13]. Metal oxide NPs including zinc oxide (ZnO) and titanium dioxide (TiO₂) are reported to enhance the asphalt mixture's resistance to rutting and cracking [13,14]. Inorganic NPs such as silica (SiO₂), carbon nanotubes (CNTs), and nano-clay are seen to have excellent potential in the reinforcement of asphalt materials and improving their durability [15,16]. The rheological performance of bitumen – and consequently the performance of the corresponding asphalt mixture – was successfully improved through the addition of SiO₂ NPs. The thermal and mechanical stabilities of the asphalt mixture were also improved by incorporating clay NPs [17,18]. To the best of our knowledge, clay and silica families are the most widely used inorganic NPs to improve the binder resistance to aging [19-22]. Clay and silica families were reported to be one of the excellent inorganic NPs in improving binder aging properties. Based on the results of different reports, nano-silica-modified asphalt binders slightly decreased viscosity and complex modulus, while improving fatigue and rutting resistance after short-term aging [19-21]. In addition, some investigations have shown that nano-silica-modified binder has a higher resistance to thermal aging, ultimately leading to increased durability of asphalt pavements [21,22]. SiO₂ NPs have advantages such as nonphotocatalytic, inorganic shielding, and nontoxic, which are of crucial importance for use in asphalt mixtures [23,24]. However, fumed SiO₂ NPs are one class of synthetic nanomaterials that has environmentally friendly and economic justification to use on large scale. Fumed silica is a synthetic amorphous structure nanomaterial with a large surface area and nano-size scale [25]. Therefore, this study focuses on clay/fumed silica nanoparticles (CSNPs).

In comparison to the conventional way, warm mix asphalt (WMA) technology works in an efficient eco-friendly

manner. In this case, asphalt is produced at a temperature of approximately 30–60°C, which is lower than usual. This technology reduces the emission of harmful vapors and leads to 20-35 and 35% less greenhouse gas emissions and energy consumption, respectively [13,26]. However, moisture susceptibility is a common disadvantage of WMA technology, leading to a decrease in its performance [27,28].

The objective of this research is to identify the potential impacts of CSNPs on the aging resistance of road asphalt binders that are used for road asphalt mixtures produced by WMA technology. In detail, the morphological, chemical, thermal, rheological, and mechanical properties of CSNP-modified asphalt binders are meticulously analyzed in various conditions. New insights are presented toward a further understanding of potential changes in mechanical and rheological binder properties due to thermal aging. Figure 1 schematically illustrates the experimental techniques applied in this study.

2 Materials and methods

2.1 Materials

The synthesis process of CSNPs was selected according to the authors' previous research (as shown in Figure S1) [29]. Nano fumed silica (Aerosil A300, Degussa Co., Germany), sodium bentonite (Sigma Aldrich Ltd., Germany; see Table S1), and Bitumen 50/70 (Total Co., France) were used in this research. The particle size analysis of materials was performed using a dynamic light scattering (DLS) (Malvern ZEN 3600, UK), while X-ray diffraction (XRD) analysis was conducted using an X-ray powder diffraction (Philips PW 1730, Netherlands; Figure S2). To prepare the WMA mixture, a new formulation of Fischer-Tropsch (FT) wax (Sasol, South Africa; Evonik, Germany; Sigma-Aldrich, Germany) was synthesized in this investigation. Before use, nanocomposites were dried in an oven at 110°C for 3 h. In the first step, samples were prepared in accordance with prior works procedures [18]. Subsequently, nanocomposites were added to bitumen in different quantities (0.1, 2, and 3 wt%). In this study, bitumen was modified using a 3% WMA additive. This value was chosen based on the commonly used wax content used in WMA mixtures reported in the previous study [13].

2.2 Aging process

For the rolling thin film oven test (RTFOT), according to ASTM D1754, samples were kept at 163°C in the rolling

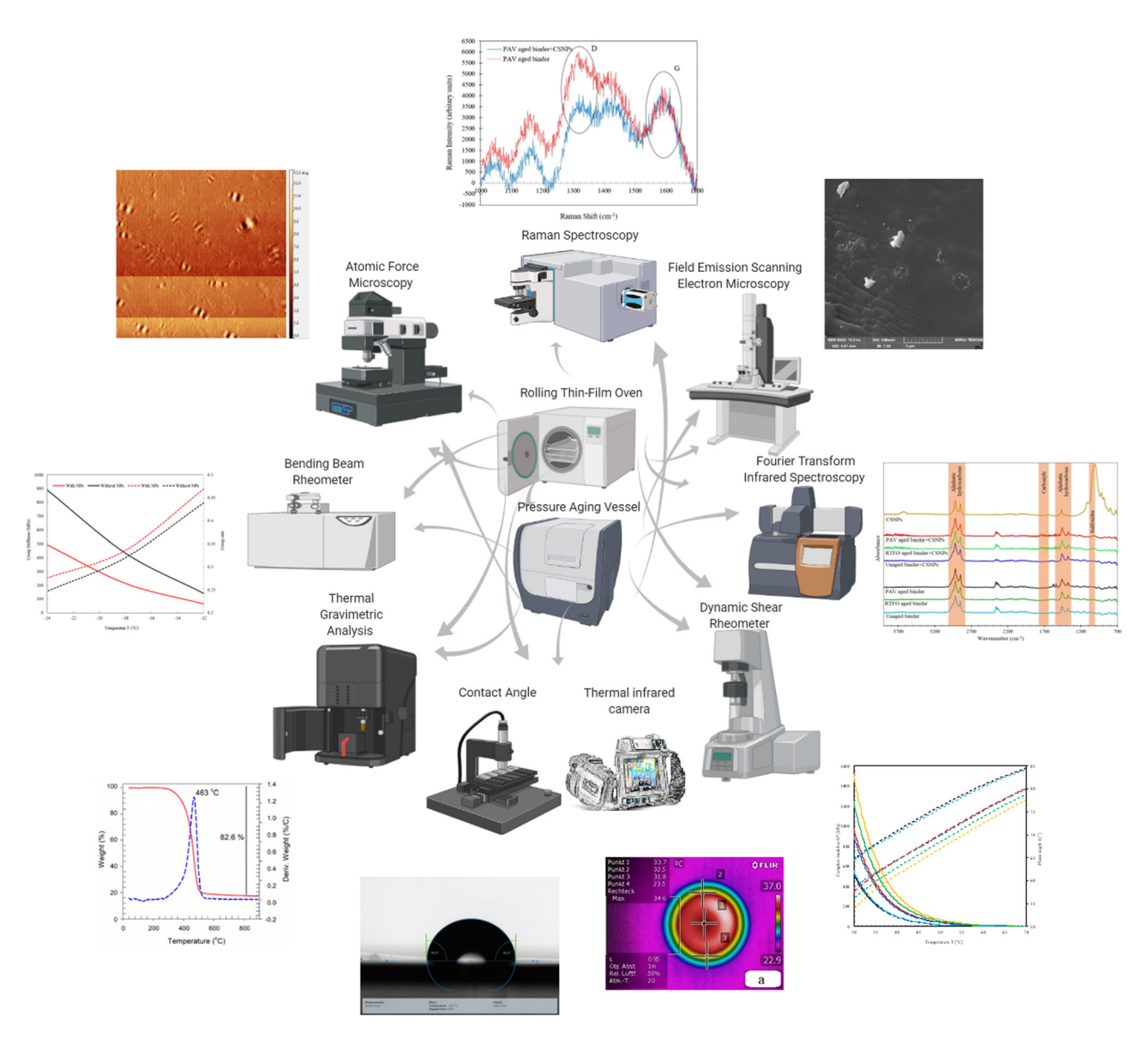


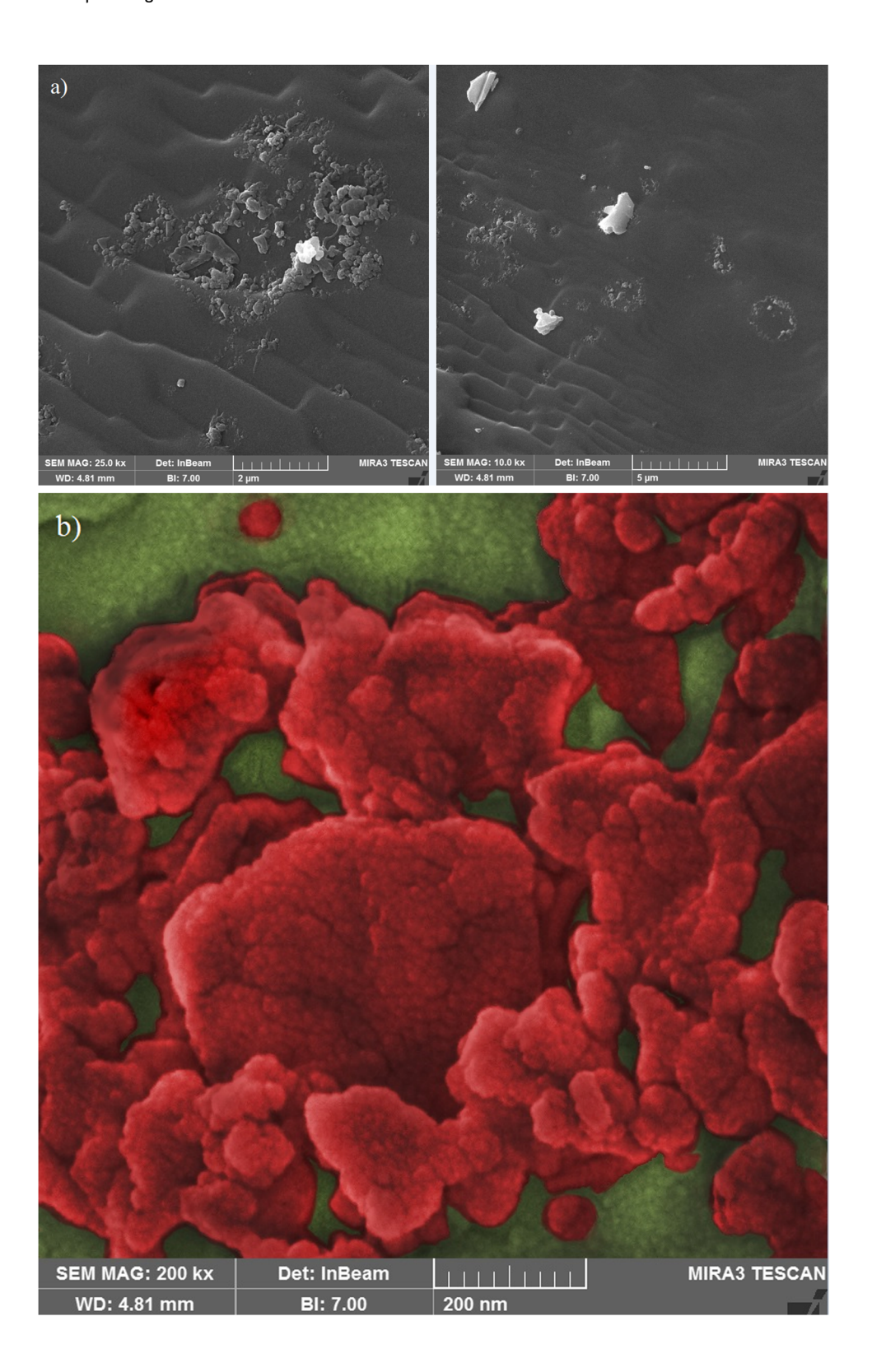
Figure 1: Schematic overview of experimental techniques applied in this study.

thin-film oven (RTFOT 8, model of ISL, France). Based on the pressure aging vessel (PAV) standard procedure, samples were investigated in the PAV after long-term aging (with a 300 psi and 100°C for 20 h). We prepared samples in three conditions: S1–S4: unaged samples, S5–S8: short-term aged samples, and S9–S12: long-term aged samples. All the samples are presented in Table S2 (Supplementary materials).

2.3 Characterization methods

A dynamic shear rheometer (DSR) device (Malvern Kinexus Pro+, UK) was applied to evaluate the rheological properties at a frequency of 10 rad/s and temperature between 20 and 70°C. The phase angle and complex shear modulus

 (G^*) of base asphalt binder and aged samples were measured according to the standard AASHTO T 315. This method is generally used for characterizing asphalt binder properties in the linear viscoelastic range. Chemical properties were tested using Fourier transform infrared (FTIR; Thermoscientific Nicolet iS10, USA) and a TG/DTA (SDT Q600, TA Ins., USA). A Renishaw inViaTM confocal Raman microscope (Renishaw plc, Miskin, Pontyclun, UK) with an argon laser source (633 nm) was used to study chemical bonding and aromatic sheet size, which was equipped with a charge-coupled device detector (4/cm spectral resolution, 90° scattering geometry). The survey spectrums were recorded ranging from 500 to 3,000/cm at room temperature (50× long work distance objective). Atomic force microscope (AFM; Nanowizard, JPK Ins., Germany) with cantilevers in a



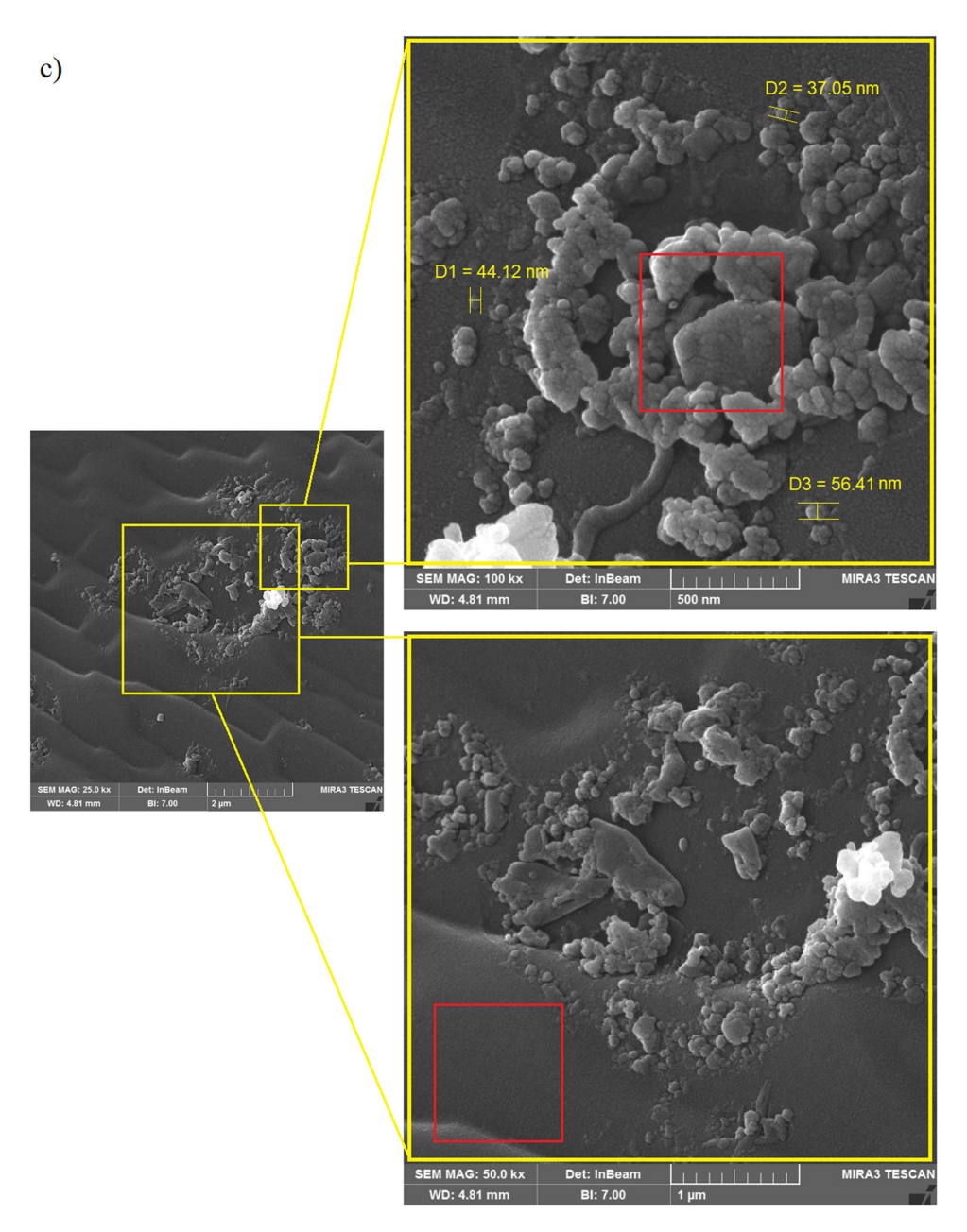
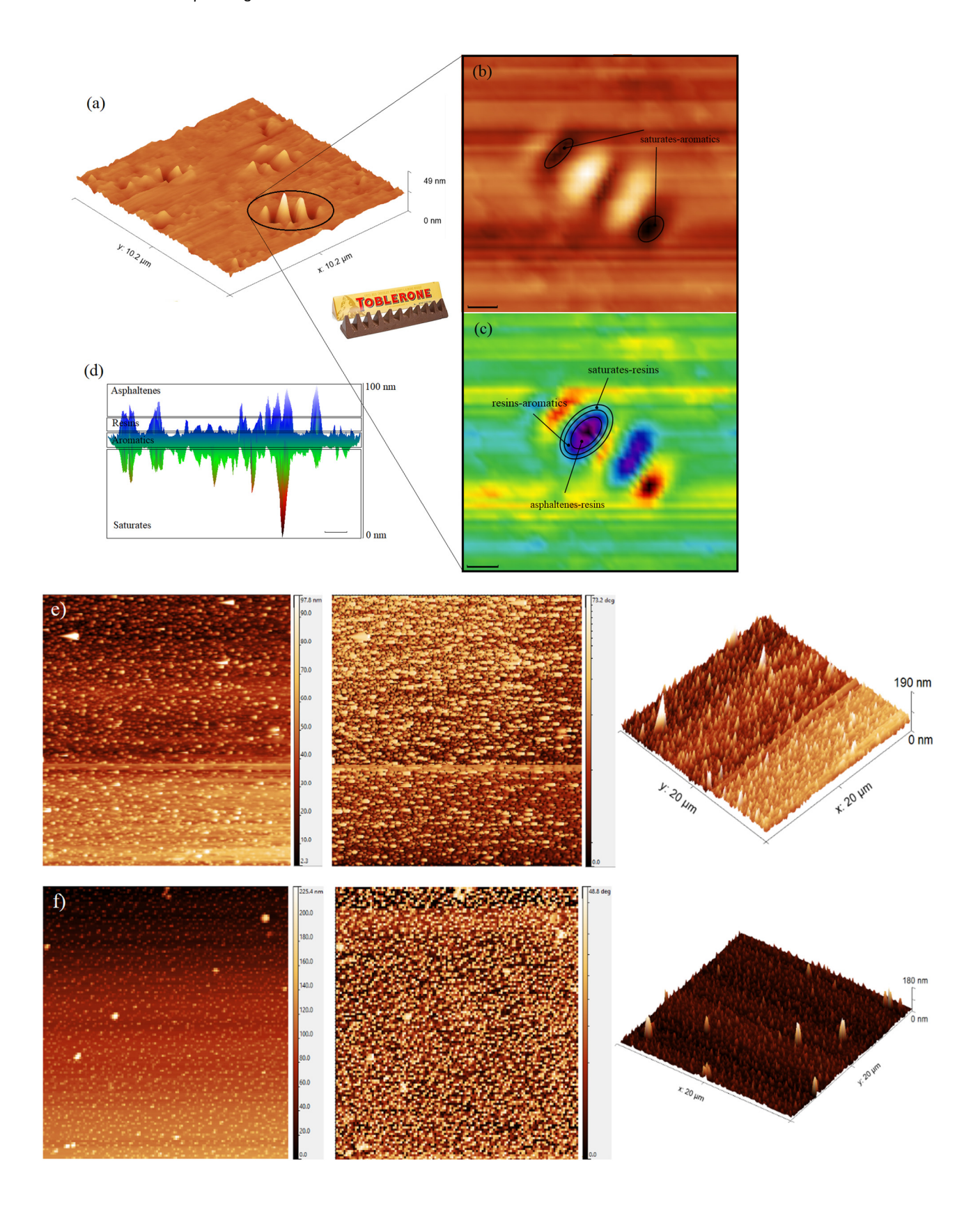


Figure 2: (a) FESEM images of asphalt binder modified by CSNPs at different magnifications. (b) FESEM colored images of CSNPs on binder surface; CSNPs coat a large surface of the binder due to the high surface area-to-volume ratio (one of the unique physical properties of CSNPs). The red shows an aggregation of NPs, and green demonstrates the asphalt binder surface. (c) FESEM images of asphalt binder surface at different scales and aggregation sizes of CSNPs. The first red square illustrates the aggregate of CSNPs, and the second red square shows the surface of the asphalt binder. The average size of CSNPs is 45 nm.

tapping mode (RTESP, Bruker, USA) and field emission scanning electron microscope (FE-SEM; TE-SCAN, MIRA III, Czech Republic) were used to study morphology and structures of binder samples in microscales and nanoscales. Roughness and thickness map images at 1–2 frames/s and a set-point z were analyzed, and the results were evaluated using the open-source software Gwyddion [30]. The morphologies were characterized by focusing an electron beam on the

surface of the binder samples. A thermal infrared camera (FLIR-T440, US) recorded thermographic images in specific time steps from binder samples. Flexural creep properties at low temperature were analyzed by using a thermoelectric bending beam rheometer (TE-BBR; Cannon Ins., USA). In this study, we used Petrotest[©] for softening point (PKA5, Germany), automatic penetrometer (PNR 12, Germany), and ductility test (infratest, 20-2356, Germany). A summary



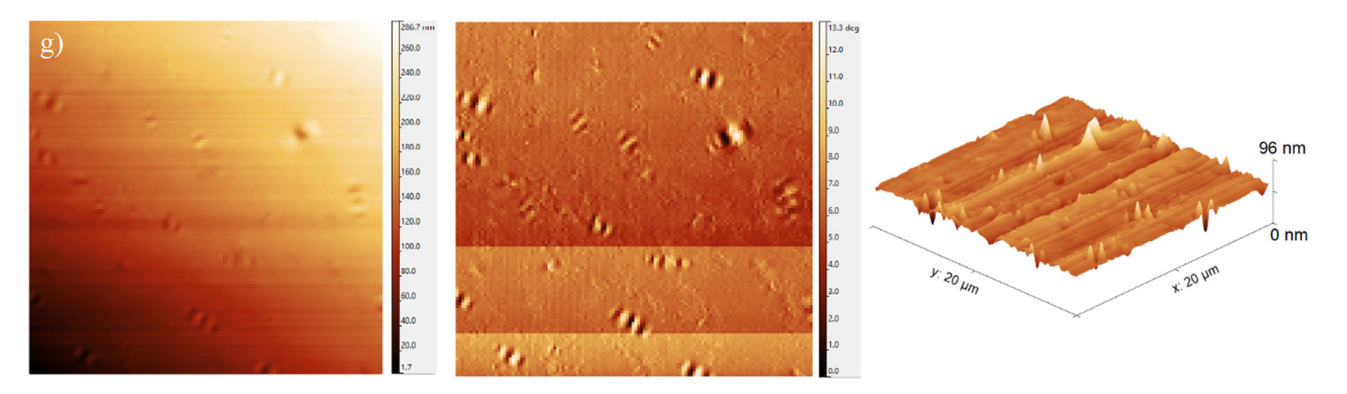


Figure 3: (a) AFM 3D view of the surface morphology of asphalt binder, showing bee-like structures after aging that looks like a Toblerone chocolate bar; the bee-like structure is affected by the polarity of asphaltene molecules and is a challenging phenomenon that is directly related to long alkyl chains of asphaltenes, high aromatic components, and microcrystalline waxes. Aging affects the size of the individual bees and their number on the binder surface considerably, and with the increasing size and number, the binder surface stiffness increases. (b) AFM 2D view of components of bee-like structures. (c) Colored single bee; red zone represents saturates—aromatics, violet zone shows asphaltenes—resins, dark blue zone illustrates resins—aromatics, and light blue zone shows saturates—resins content. The scale bar is 500 nm. (d) 3D cross-section of asphalt binder and four components of asphalt binder: asphaltenes, resins, aromatics, and saturates. The scale bar is 1 µm. 2D and 3D AFM surface images of binders: (e) morphological unaged sample, (f and g) short-term and long-term aged samples, respectively; at three different modes: center row, phase image; left and right rows, 3D and 2D surface topography samples.

of the physical characteristics of the asphalt binder used in this study is presented in Table S3 (Supplementary Materials).

3 Results and discussion

3.1 Surface morphology

FE-SEM was conducted to observe the surface morphology of CSNP-modified asphalt binder samples in the asphalt binder matrix (Figure 2a). FE-SEM images display uniform dispersion of CSNPs (average particle size ~45 nm) in the asphalt binder matrix. Unique nanolayer shapes of CSNPs in asphalt binder matrix significantly affect the aging process: like a shield. In this case, CSNPs prevent the upper structure from destruction through radiation [8] and simultaneously trap volatile compounds and prevent evaporation from the asphalt binder.

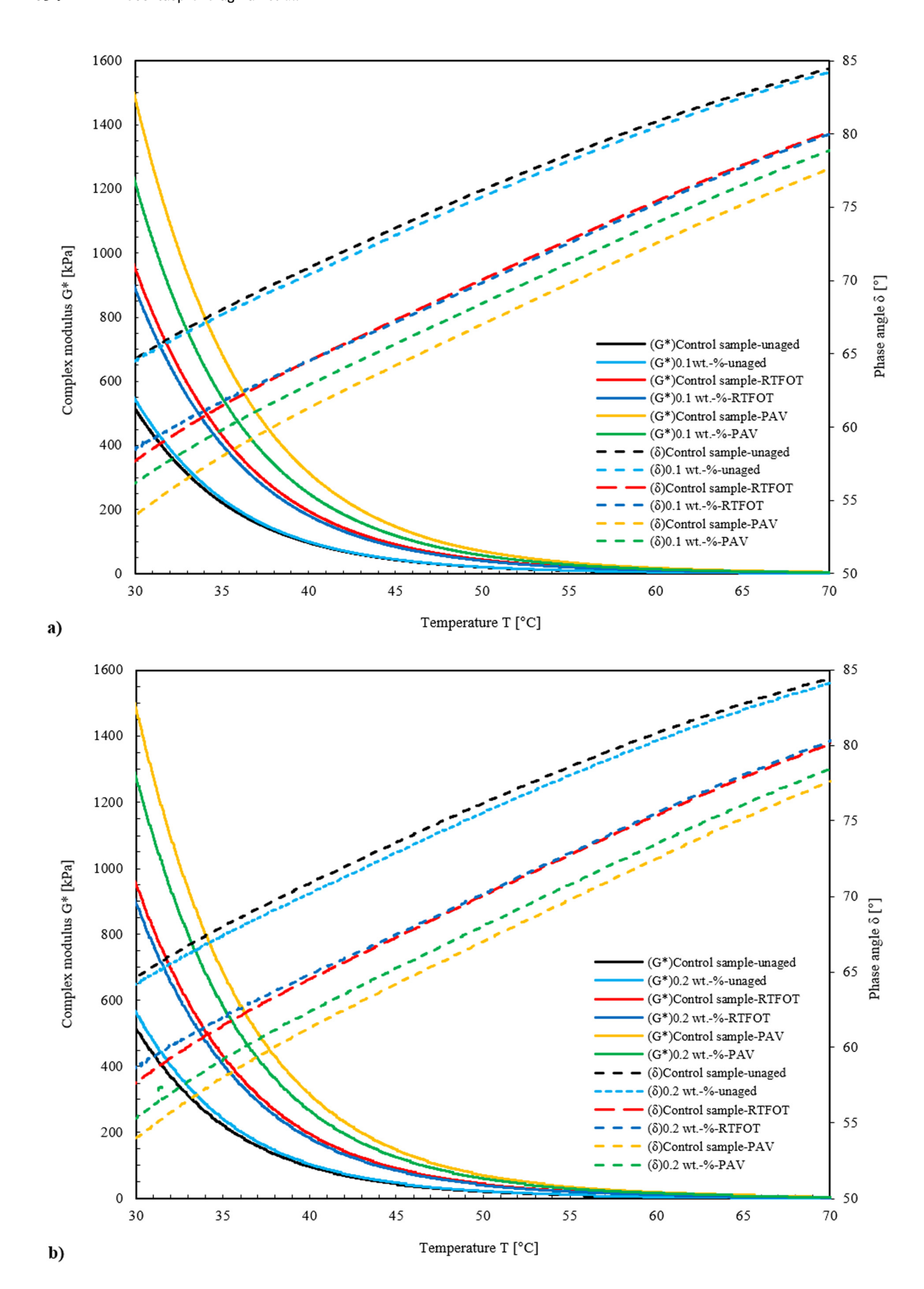
Due to their large surface area, clay nanolayers and fumed silica NPs coat a wide area. To use this feature, suitable dispersion of CSNPs in asphalt binder is essential. Distribution can be analyzed (see Figure S3) using energy-dispersive spectroscopy (EDS). The elements aluminum, silica, iron, and titanium can be detected and used to identify the distribution of CSNPs in base binders. Clay layers in binders' surfaces are usually detected *via* titanium dioxide (with 1 µm average particle size). The

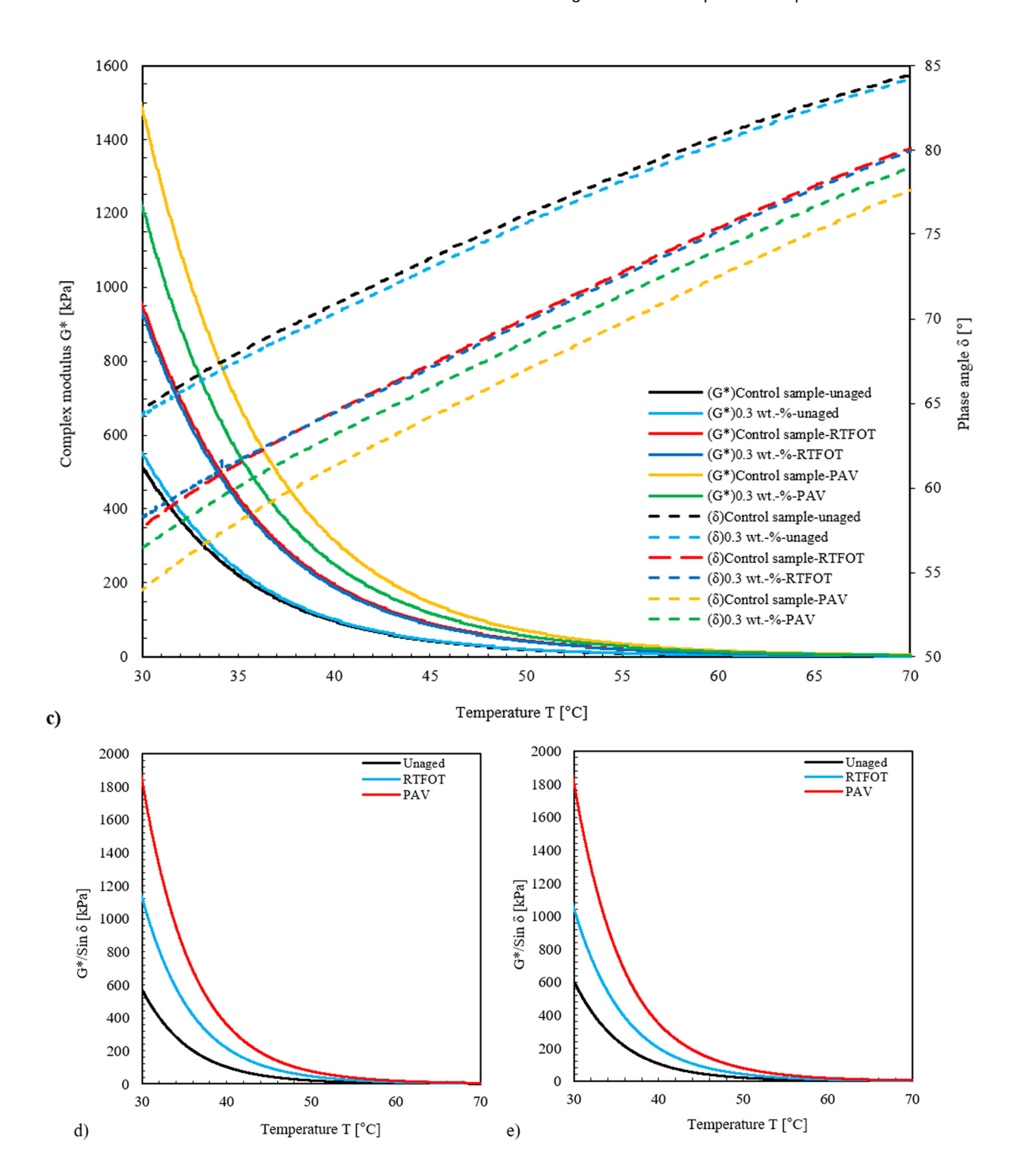
map of titanium elements shows that the distribution of the particles in bitumen is uniform.

The nanostructure formed by CSNPs acts as a nanoshield against oxidation and thermal destruction. Clay layers are of high heat resistivity and avoid decomposition of chemical bonds and thus delay binder aging [8]. Figure 2b and c shows the partially uniform cover of CSNPs on asphalt binders (green color) and dense bulks of CSNPs (red color), respectively. Polarity and chemical bonding [31,32] are important parameters that cause nanolayers to adsorb together and create these bulky components in asphalt binders.

To further understand the effect of CSNPs on the binder, morphological properties were analyzed through the AFM test. The identification of the change of the binder microstructure due to aging is of interest because it shows the changing molecular interactions and chemical compounds [33,34]. The microstructures of binder samples modified by CSNPs are shown in Figure 3.

In Figure 3, three phases Catana, Peri, and Para are shown that indicated bee-like structures, dispersed phase, and smooth matrix phase, respectively. The Catana and matrix phases are considered as microstructure characteristics of the binder [35]. Bee-like structures are attributed to the long chains of alkyl in microcrystalline waxes, aromatics structures, and asphaltenes, which crystallize during cooling [36]. Bee-like structures in AFM images indicate the possible presence of asphaltic components (Figure 3b–d). The amount of asphaltenes and colloids is directly related to the size of the bee-like structure in the





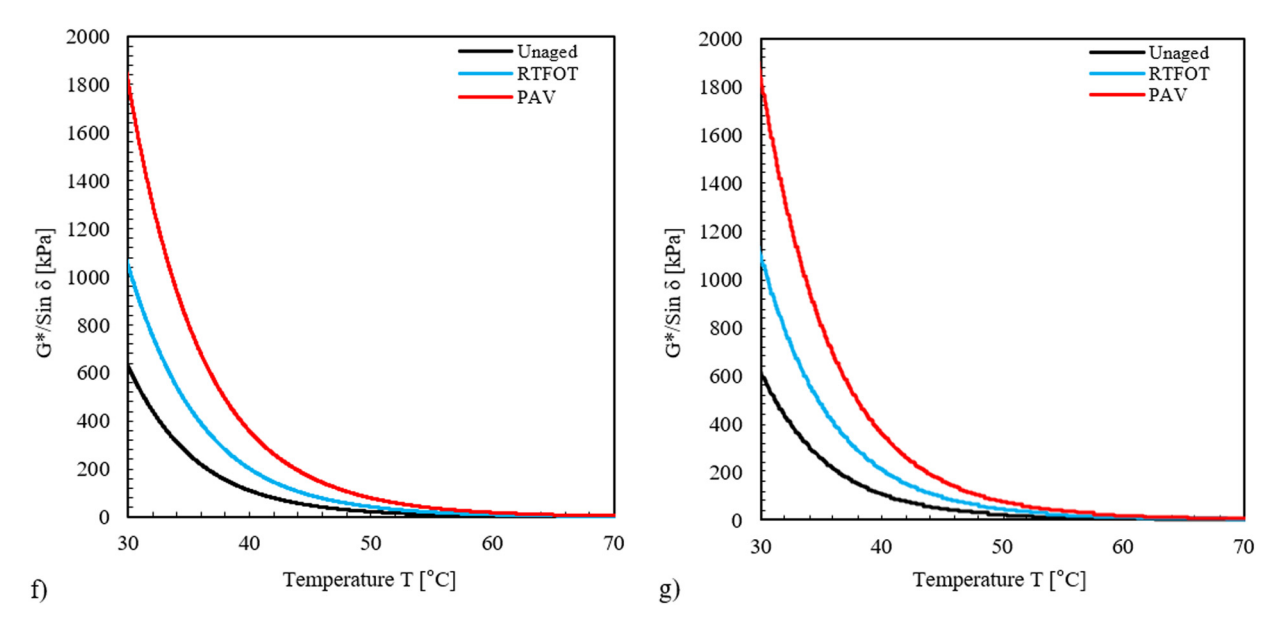


Figure 4: Phase angle and complex modulus of modified asphalt binder, (a) 0.1 wt%, (b) 2 wt%, and (c) 3 wt% CSNPs. Rutting resistance of CSNP-modified binder in short- and long-term aged and unaged conditions for (d) base samples, (e) 0.1 wt% CSNPs, (f) 0.2 wt% CSNPs, and (g) 0.3 wt% CSNPs.

asphalt binder; the larger the structure, the higher the number of asphaltenes and colloids [37]. The microstructure morphology and the individual phases of short- and long-term aging binder samples are presented in Figure 3e–g. The comparison of AFM images of long-term aged and virgin samples illustrates the disappearing nanostructure and the increasing formation of bee-like structures. The same process can be observed on Videos 1–3 (see Supplementary Materials), recorded during the AFM measurements, which show the consequential structural change of binder aging. The addition of CSNPs to the asphalt binder leads to significant changes in binder morphology and microstructure. These changes explain the role of CSNPs as a shield to binder aging.

3.2 Dynamic viscoelastic properties

Viscoelastic properties of binders were analyzed by the DSR test. The phase angle (δ) and the corresponding

complex shear modulus (G^*) were measured over the frequency range (10 rad/s) and a large temperature (from 20 to 90°C). The binders' resistance to deformation (rutting) permanent (plastic) was investigated according to parameter G^* /sin δ parameter [38]. The results are illustrated in Figure 4a–c. Deformation resistance of asphalt binder is considered with phase angle and complex modulus, which loading frequency and temperature parameters have the main effect on G^* and δ [8].

The sample with CSNPs in an amount of 0.2 wt% shows the highest deformation resistance before aging. Aging leads to an increase in stiffness. The maximum level of stiffness is always observed for aged base samples, which is linked with an increase in elastic behavior [39] and disadvantageously with an increase in brittleness [40]. The complex modulus conditions change upon the addition of NPs to the asphalt binder. For CSNP-modified samples, the increase in stiffness upon aging is less distinct due to the reinforcing effect of NPs. Based on the results of this study, the addition of 0.2 and 0.3 wt% of

Table 1: Threshold temperatures of asphalt binder before and after aging in various concentrations (S1-S12) of CSNPs

Threshold temperatures (°C)											
	Before aging	After aging $(G^*/\sin \delta = 2.2 \text{ kPa})$									
S1	S 2	S 3	S 4	S 5	S 6	S 7	S8	S 9	S10	S11	S12
72.8	73.0	73.4	73.1	73.0	72.4	72.9	72.7	77.4	77.4	77.6	78.0

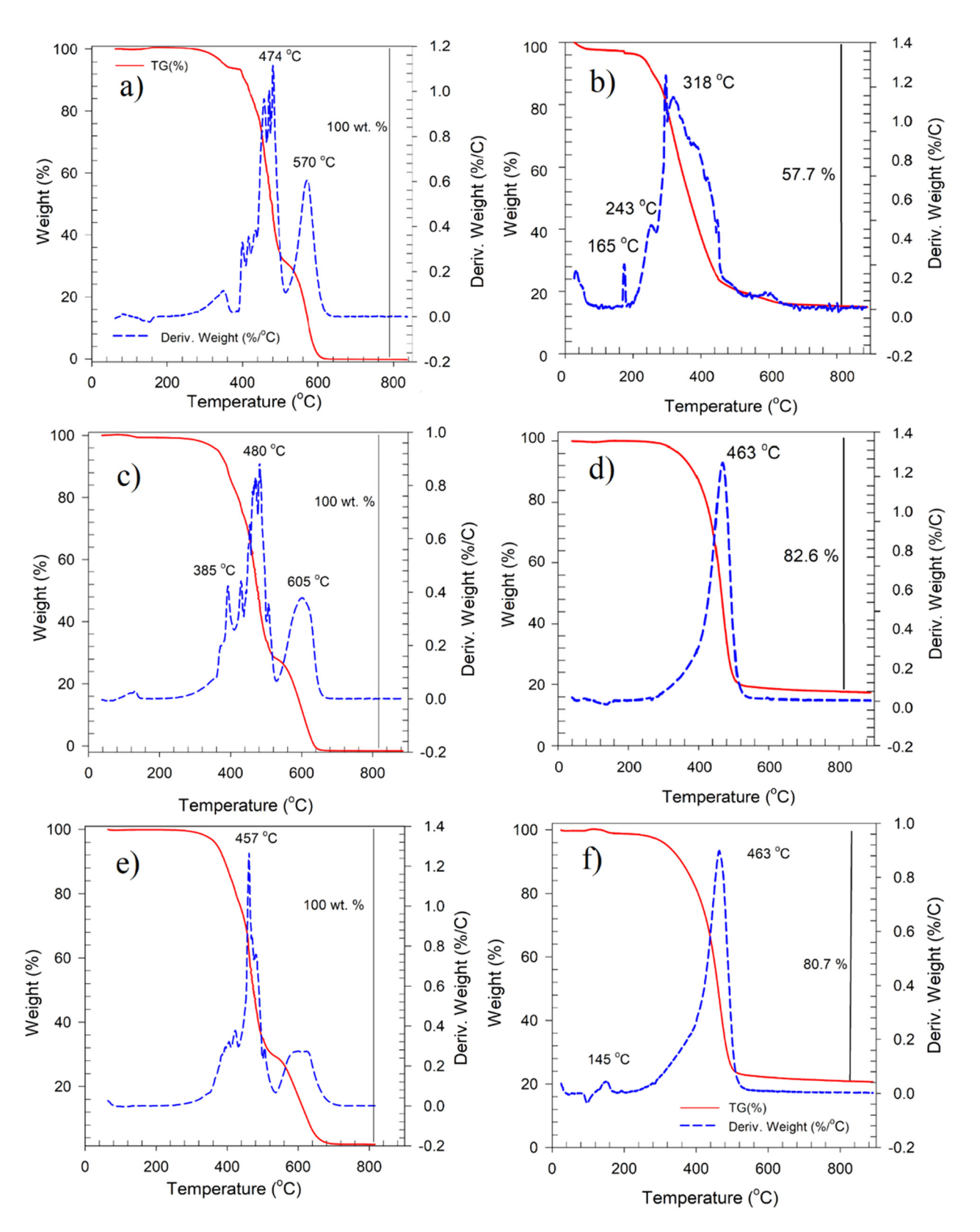


Figure 5: Derivative thermo-gravimetry and thermal gravimetric analysis images: unaged binder samples: (a) base samples and (b) CSNPs modified; short-term aged binder: (c) base samples and (d) CSNPs modified; long-term aged binder: (e) base sample and (f) CSNPs modified.

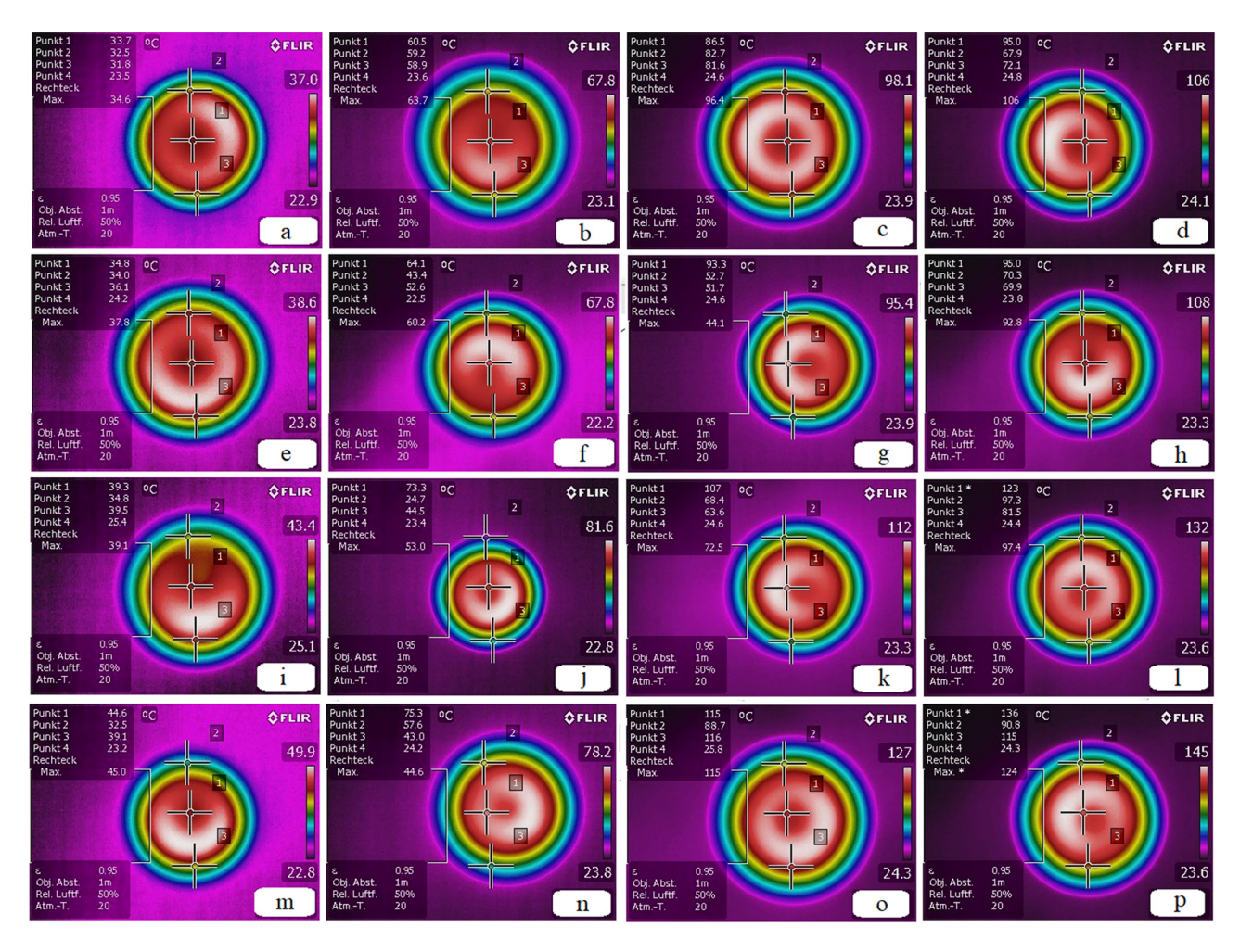


Figure 6: Infrared thermal image: WMA additive (a-d) with CSNPs, (e-h) without CSNPs; without WMA additive (i-l) with CSNPs and (m-p) without CSNP; in different thermal zones: (d, h, l, p) 120 s, (c, g, k, and o) 90 s, (b, f, j, and n) 60 s, and (a, e, l, and m) 30 s. The sample's diameter is 18 mm.

NPs to the asphalt binder shows the highest resistance to permanent deformation after short- and long-term aging, respectively. An optimum content of CSNPs in the asphalt binder can be determined for obtaining CSNP-modified binders with the highest resistance to aging. After PAV aging, the phase angle and complex modulus ranking were 3.0 wt% NPs < 1.0 wt% NPs < 2.0 wt% NPs < 0.0 wt% NPs, and 0.0 wt% NPs > 2.0 wt% NPs > 1.0 wt% NPs > 3.0 wt% NPs, respectively.

In Figure 4d–g, rutting parameters before and after aging are displayed (at 30 and 70°C). Samples 6 and 12 demonstrated the most distinct improvement after short-and long-term aging, respectively. The results show the resistance to permanent deformation, which improved upon the addition of CSNPs.

In this investigation, the efficiency of rutting resistance is considered with the threshold temperature of the rutting factor. Table 1 presents a threshold temperature of

1.0 before aging and 2.2 kPa after aging (based on SHRP-A-369 standard [38]). The results show that CSNPs decrease rutting resistance before aging. After aging, the threshold temperature and hardening of base samples increase, while the contrary is measured for CSNP-modified samples. These observations confirm that CSNPs reduce the stiffness and hardening due to aging. Moreover, the results showed that 0.1 wt% of CSNPs performs higher in comparison to 0.2 wt%.

3.3 Thermal and spectroscopy analysis

Thermogravimetry/differential thermal analysis (TG/DTA) was carried out to investigate the thermal stability and the pattern of thermal decomposition. Figure 5 shows the results of thermogravimetric analysis (TGA), where the weight loss of the samples is measured with the increasing temperature up to 900°C.

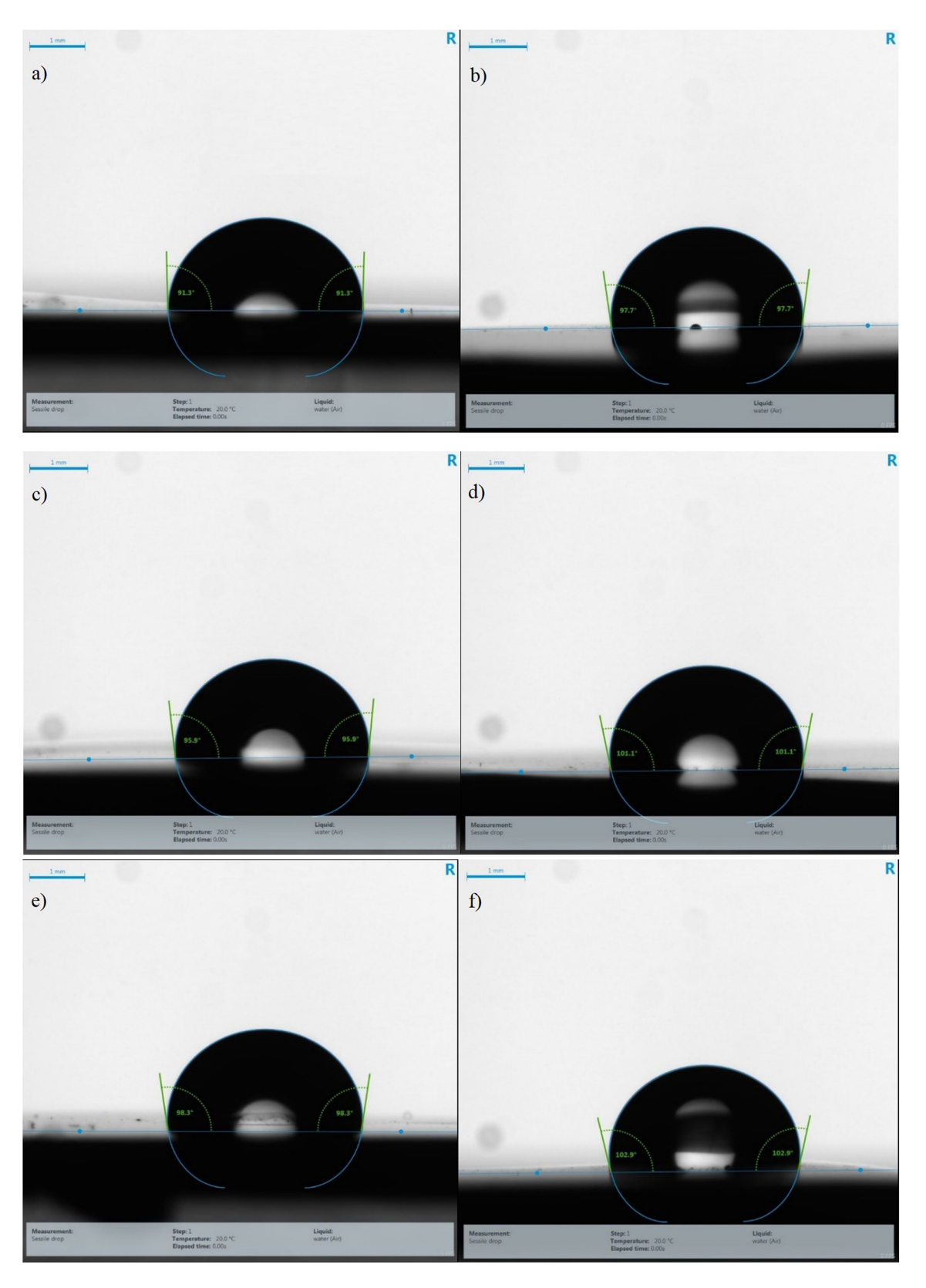


Figure 7: Contact angle images: unaged binder (a) without CSNPs and (b) with CSNPs; short-term aged binder (c) without CSNPs and (d) with CSNPs; long-term aged binder (e) without CSNPs and (f) with CSNPs.

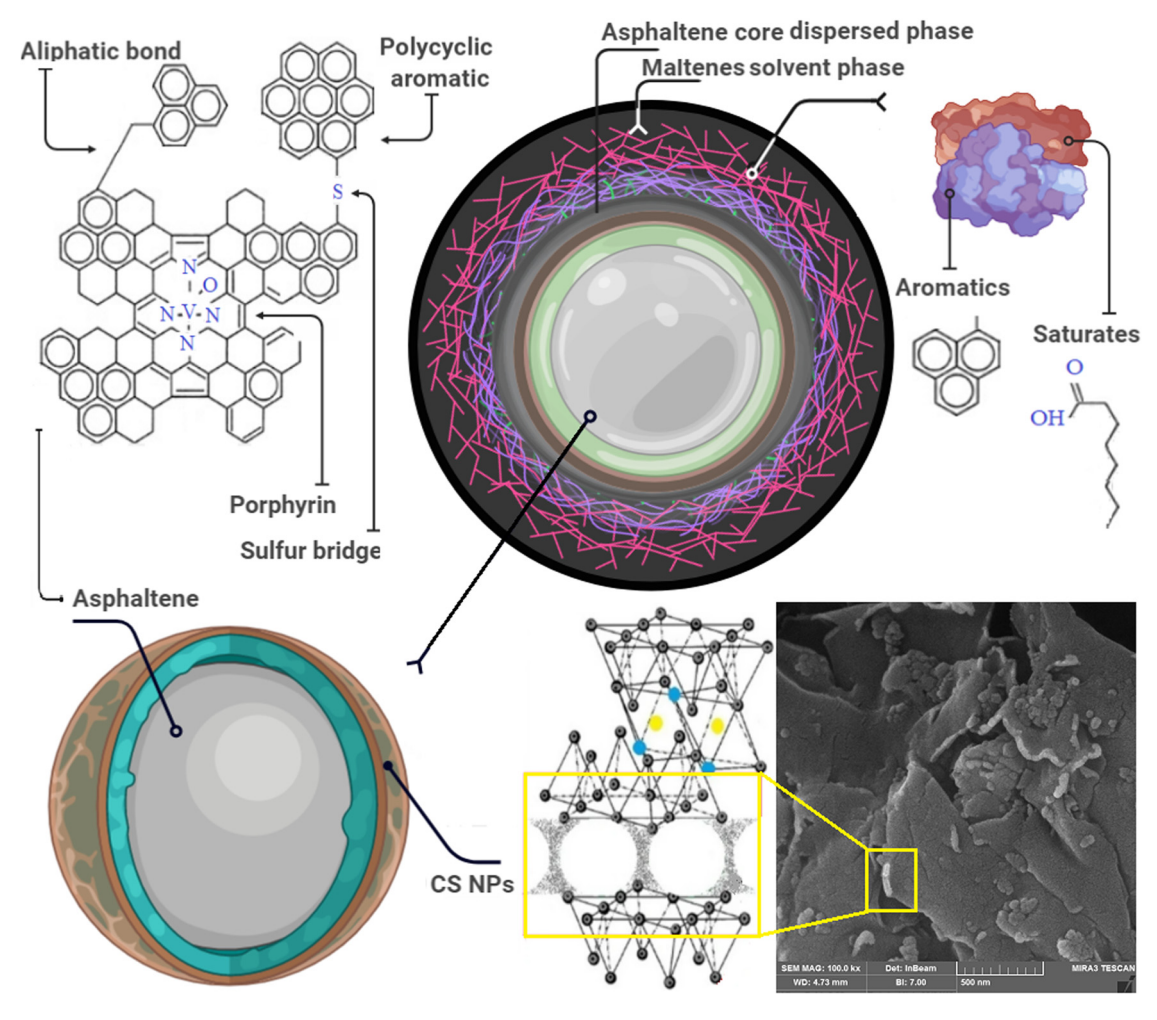


Figure 8: Schematic of action of clay/silica NPs and bitumen compositions.

Three main ranges of mass loss are shown in thermal decomposition: temperature ranges of 200–360, 370–490, and 540°C. Over the temperature range of 480–580°C, heteroatom bonds of base samples are decomposed, and resins are oxidated and dehydrogenated. In the next stage, the polymerization/cracking process produces asphaltenes that increase the binder weight loss [41,42].

CSNP-modified binder samples have increased thermal stability. The final decomposition in CSNP-modified binders happened sooner in comparison to base samples that this subject may be related to fumed silica NPs (Figure S4). The carbon residue of base samples arrives at zero at 800°C (maximum mass loss); however, there is a 20–43% carbon residue in the CSNP-modified binders. The CSNP-modified binders with lower weight loss have higher heat stability and lower evaporation [43]. Most of the mass loss for CSNPs binder samples occurs at temperatures above 200°C, which is much higher than the operating temperature required for

asphalt mixtures; therefore, this nanocomposite has acceptable thermal performance in asphalt binders.

The temperature distribution on the sample surface during 120 s at different times (by using infrared thermal images) – always calculated by chosen three points on the surface [44,45] – is shown in Figure 6. Temperature changes are shown by the color change in asphalt binder samples. At low temperature (Figure 6a, e, i, and m), heat distribution is uniform; however, temperature increases from 44.6 to 136, 34.8 to 95, and 33.7 to 95°C for the sample without WMA additive, with WMA additive, and with WMA additive + CSNPs after 120 s, respectively. Figure 6 shows that without WMA, additive samples have linear heating rates and a growing surface temperature trend. Figure 6h and p shows that WMA samples can release uniformly heat; however, base samples create heat accumulation. In addition, WMA samples have a more suitable temperature distribution than base samples at a

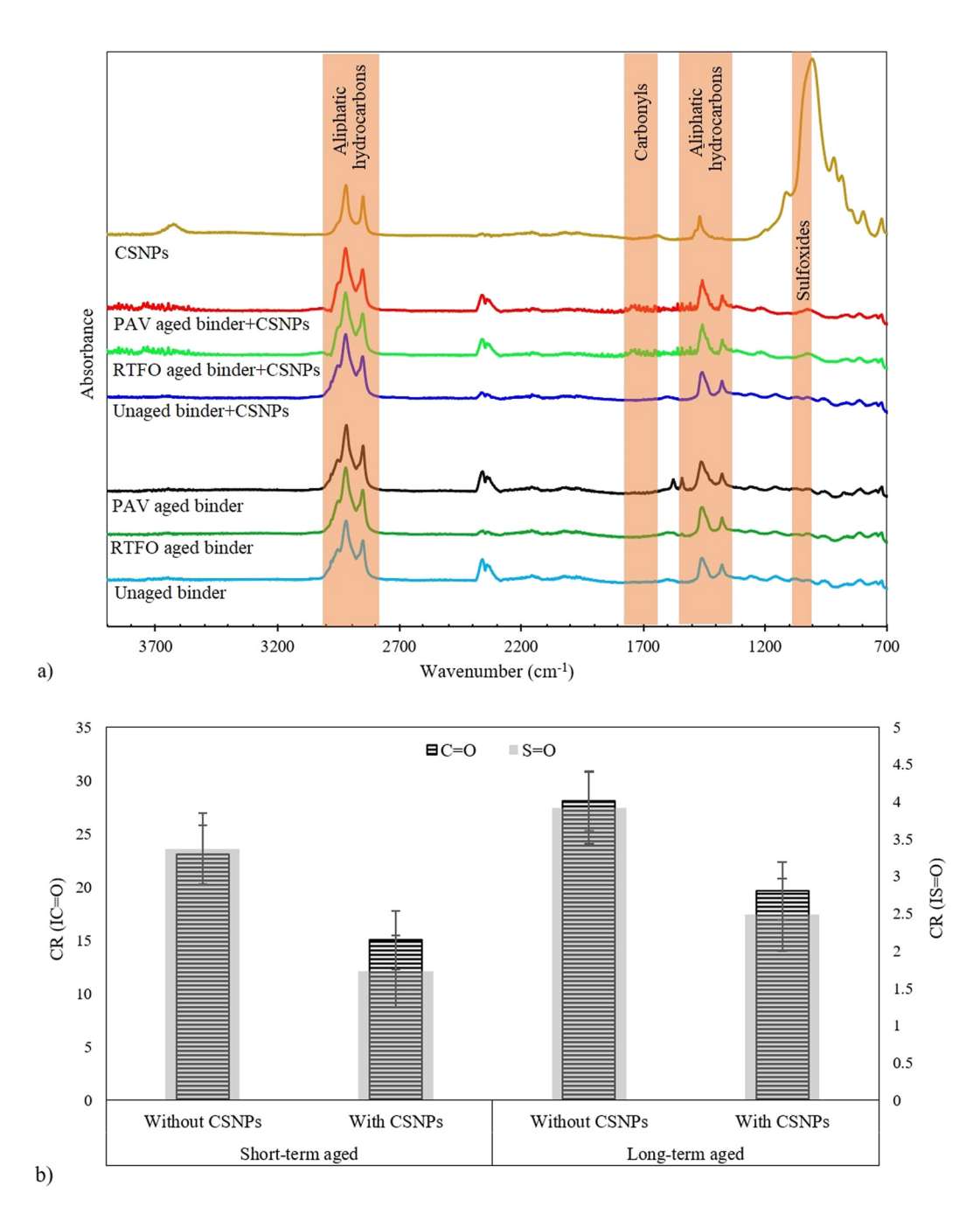


Figure 9: (a) FTIR spectra of asphalt binders at different aging conditions (wavenumber 700–4,000/cm) and (b) sulfoxide and carbonyl aging indexes at different aged conditions.

lower heat level. Figure 6a–d and i–l shows the released heat rate of samples without and with CSNPs, which are 0.63 and 0.62°C/s, respectively. These figures indicate that WMA additives with and without CSNPs have similar thermal mechanisms.

The comparison of temperature distributions of samples modified by CSNPs and fumed silica NPs (Figure 6 and Figure S5) shows that the effect of CSNPs on WMA is more effective than fumed silica NPs. In addition, the

sufficient performance (temperature distribution) of samples modified with silica NPs and clay NPs indicates the self-healing phenomenon in the asphalt binder [46,47].

3.4 Contact angles of asphalt binders

Figure 7 shows contact angles (CAs; between water and asphalt binder surface) for various asphalt binders before

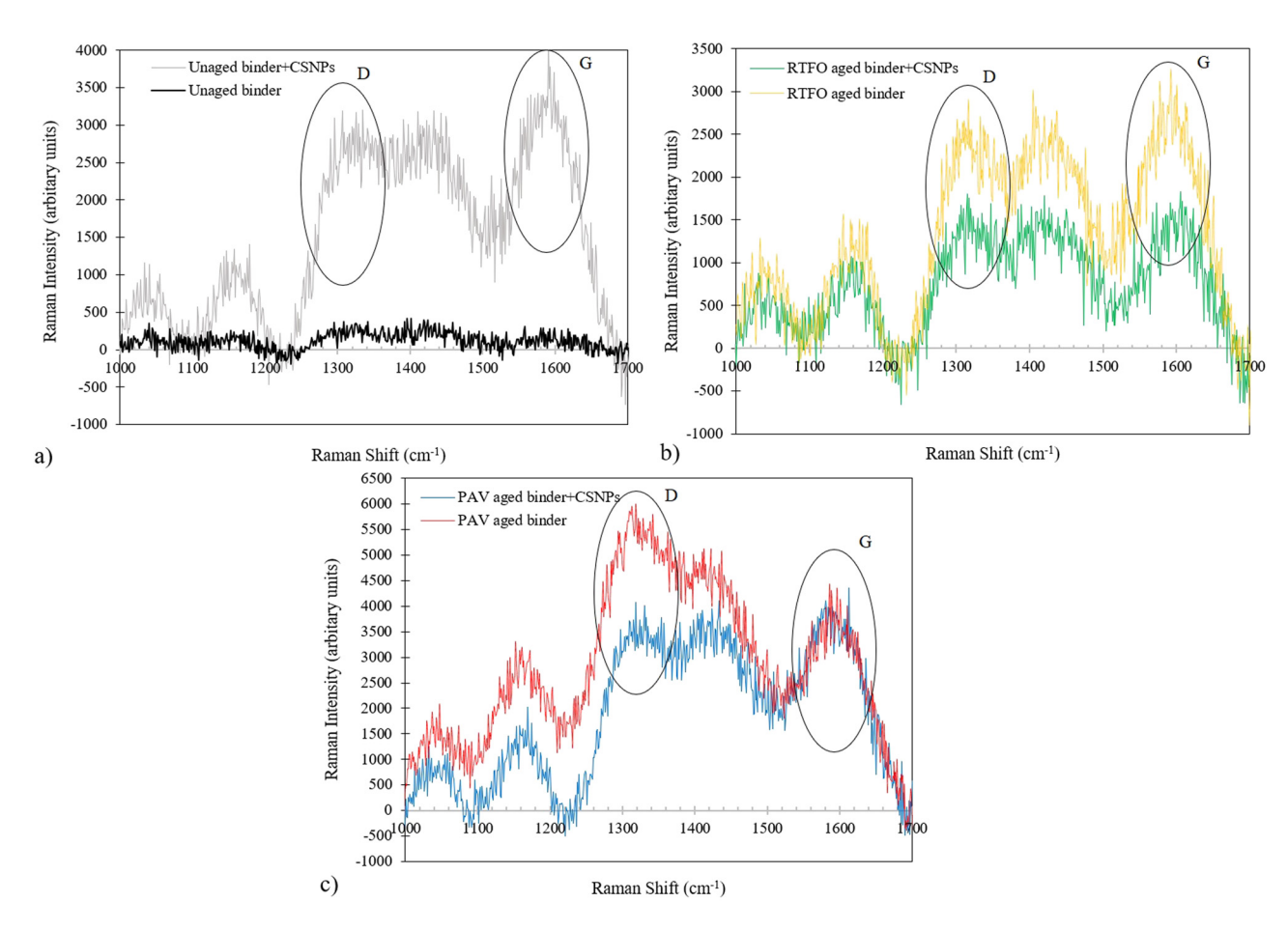


Figure 10: Raman spectra of the binder samples: (a) unaged, (b) short-term aging, and (c) long-term aging.

and after aging. CA values higher or lower than 90° show hydrophobicity or hydrophilicity of the samples, respectively. CSNP-modified samples are more hydrophobic, and thus, fewer water molecules are trapped in the binder surface. To put it another way, CSNPs significantly reduce residual molecules of water in the asphalt mixture and alter the wettability of asphalt binders. This phenomenon indicates that CSNP-modified binders have much higher moisture susceptibility in comparison to the base binder samples. Videos 4–6 (see Supplementary Materials) compare CAs of modified samples before and after aging.

In Figure 7, the increase in CA from 91 to 97° of a CSNP-modified sample is shown. This observation could be related to the hydrophobic nature of fumed silica NPs. The ratio of fumed silica NPs in asphalt binder could play a key role in binder wettability (CAs of fumed silica NPs are shown in Figure S6). In addition, CA imaging showed that for increased aging levels, a slight increase (from 6 to 7°) in CA long-term aging is observed.

3.5 Mechanism of CSNPs and bitumen

Several mechanisms affect the anti-aging process of asphalt binder modified by CSNPs. In this interaction, an increase in surface energy causes an increase in hydroxyl groups bonds between silica NPs and bitumen [8,48]. Besides, the high surface area-to-volume ratio of clay nanolayers increases to combine asphalt binder molecules with clay layers [49]. Bitumen molecules could be created chemical bonds with silica NPs, and also, NPs support components of bitumen by physical reactions (van der Waals force) [50]. Asphaltene plays a key role in the rheological properties of bitumen. Based on the bitumen's colloidal structure (Figure 8), oil and asphaltene are dispersed in the solvent phase. As shown in Figure 8, due to the appropriate size of the CSNPs (average particle sizes of silica particles and clay layers are about 33 and 12 nm, respectively), they are easily dispersed between these colloidal dimensions and cover the asphaltene molecules (average diameter, 0.5–40 nm [51]);

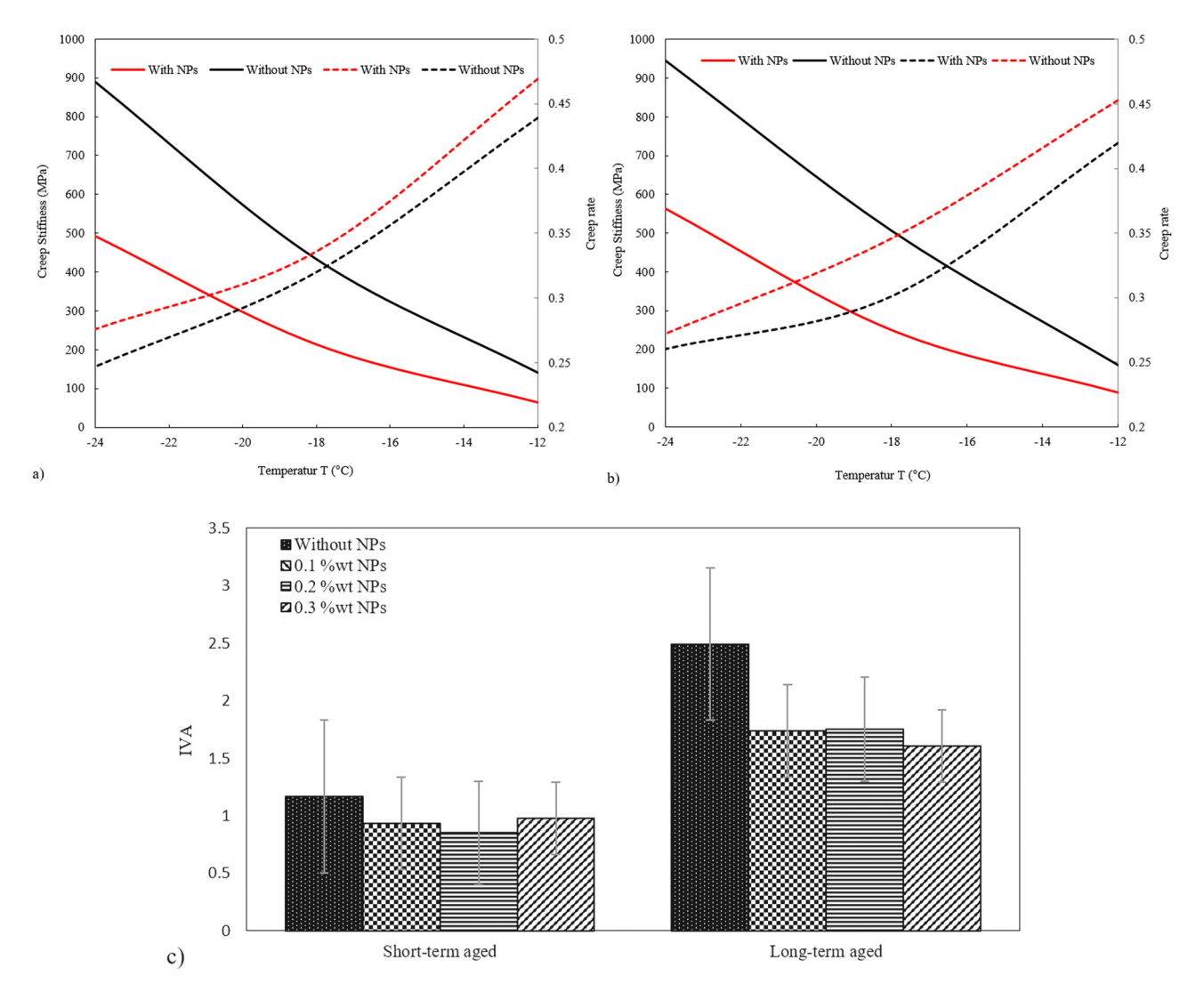


Figure 11: Creep stiffnesses (S) and creep rates (m-value) of asphalt binders: (a) nonmodified and (b) modified by NPs after long-term aging at different temperatures. (c) IVA of base binder and NP-modified asphalt binder.

hence, the mechanical and thermal properties can be modified with this molecular chemical improvement. Furthermore, nanolayers of clay have superb abilities to change the properties on the bitumen surface. Clay nanolayers are dispersed in bitumen's colloidal structure and prevent the penetration of oxygen into the matrix of bitumen at the nanoscale [52]. Other physical and chemical properties of CSNPs such as wettability alteration [53] and ion exchange reactions enhance the stability of modified bitumen and avoid decomposition of the bitumen's chemical structure.

3.6 Fourier transform infrared and Raman spectroscopy analysis

To study the chemical bonds of asphalt binder, FTIR spectroscopy was used in the range of 650-4,000/cm

(Figure 9a). Figure 9 shows the change rate (CR) of sulf-oxide and carbonyl index for short- and long-term aging. As to UV-aged samples, the carbonyl index increased more than for the base binder. The sulfoxide and carbonyl index were reduced for CSNP-modified asphalt binders. In addition, expansion of aging time increases sulfoxide and carbonyl index.

The equations in the Supplementary Materials (see Table S4) have been used to investigate chemical bonds – Aromatic (C=C), ethylene (CH=CH), carbonyl (C=O), aliphatic (C-H of CH₂)n–), and sulfoxide (S=O) indexes [54,55].

The change in the ratio of bands is shown in Figure 9b for all binder samples. During the short- and long-term aging process, carbonyl, sulfoxide, and aromatic indexes increased; however, after aging, results show that the sulfoxide and carbonyl indexes reduced for CSNP-modified binders. Due to the aging process, asphaltene is hydro-

genated into the polycyclic aromatic or hydroaromatic hydrocarbons and leads to an increase in the aromatic compounds. Conversely, after aging, due to the opposition between compounds of aliphatic and aromatic, there was a decrease in aliphatic molecules. In addition, in the CSNP-modified binder, the ethylene (CH—CH) index increased after the aging, which indicates that CSNP is an appropriate protective shield to decrease oxidative and thermal reactions [54,56]. In other words, particles of nanodiameter have an excellent capability to be used as an anti-aging shield [57].

The average size of the aromatic sheet of bitumen was determined by Raman spectroscopy (Figure 10). The Raman spectra of each sample are composed of D and G bands, except fresh bitumen [58,59]. The G and D bands show the carbon atoms $\rm sp^2$ stretching vibration within the aromatic sheet of hexagonal and the boundary of an ordered-like structure of asphaltene, respectively [58]. The band peak position of G and D ($I_{\rm G}$ and $I_{\rm D}$) in Figure 10 is in 1,585–1,599 and 1,264–1,377/cm, respectively (Figure S7) [59].

Although there are great similarities between the Raman spectra among the bitumen samples, there exist several main variations. For example, the relative proportion of aromatic rings was considerably higher in the long-term aging sample, compared with lower aromatic fused rings in the base samples. In the presence of NPs, the change in G and D band peaks can be attributed to the ability of the nanoparticle itself to change the aromatic ring interactions in the bitumen solution.

Upon closer inspection of Figure 10, adding NPs to the bitumen samples changes the intensity of asphaltene sheets. This is owed to the interactions between NPs and aromatic fused rings. The most intense peak in the D band is in the long-term aging sample, which is based on the vibrational mode of a disordered graphitic lattice with an A_{1g} symmetry [60]. Conversely, base bitumen shows that the molecules of occupied aromatic are extremely low compared to other samples due to low asphaltene aromatic sheet size [61].

3.7 Low-temperature performance and viscosity aging

The BBR test was used to calculate the creep rate (m-value) and creep stiffness (S) of asphalt binders in the function of loading time at low-temperature conditions [62]. S and m-value are key parameters for low-temperature cracking of asphalt materials [63].

In this study, *S* and *m*-value were determined for NP-modified asphalt binders at three different temperatures (Figure 11a and b). The observed creep stiffness values of NP-modified asphalt binders were reduced significantly. Hence, CSNPs improve the resistance to low-temperature cracking. Samples 7 and 11 with 0.2 wt% of CSNPs showed the most significant improvements after short-/long-term aging. The creep rate (after the aging process) decreased with the aging degree; however, nanoparticle additives significantly increased the creep rate. Fumed silica NPs improved the cracking resistance of asphalt. This owes to the fact that the NPs promote the asphalt binder surfaces and molecules, consequently decreasing aging, and in turn, modified asphalt binder samples gain sufficient elasticity at low temperatures [16,64].

Figure 11c shows the index of viscosity aging (IVA) asphalt binder samples after short- and long-term aging. The IVA is used to study the aging properties (Table S4 in Supplementary Materials).

The IVA in the NP-modified samples after short-term aging is smaller than the IVA of base samples. Thus, the aging resistance of the asphalt binder increases with NPs modification. According to the results shown in Figure 11c, the IVA is directly related to aging and increases with the duration of aging. The asphalt binder sample modified by 0.2 wt% of NPs has appropriate IVA after short-term aging, and the sample modified by 0.3 wt% of NPs has the smallest level of IVA after long-term aging. The results indicate that the IVA reduces with the increasing concentration of NPs.

4 Conclusion

The modification of asphalt binders through NPs can offer new perspectives in asphalt binder technology and might be of great use to develop the next generation of road asphalt paving materials. New types of nanocomposites might be able to significantly increase technical durability and sustainability while remaining eco-friendly and cost-effective.

This research presents the latest findings on a new nano-composite asphalt binder, modified by CSNPs. This new binder type represents considerably improved thermal, chemical, and mechanical properties when compared to conventional asphalt binders. Interesting advantages are proved in improved aging resistance and moisture resistance, reduction of asphalt mix production temperature, and improved long-term performance.

The experimental results presented in this research demonstrate that binder modification by using CSNPs change wettability advantageously and enhance the hydrophobic properties of conventional asphalt binder. Our findings show great potential to solve one of the most challenging problems in WMA technology, which is moisture susceptibility. Furthermore, detailed chemical and rheological studies indicate a significant improvement in the aging resistance of CSNP-modified asphalt binders.

Asphalt binder modification through CSNPs and WMA technology can be considered as an interesting low-cost and eco-friendly technique in asphalt pavement engineering providing novel perspectives in making asphalt materials more durable. From a broader perspective, our findings of molecular interactions between NPs and asphalt binder will open up a new avenue that will be an inspiration in the nanotechnology concept in asphalt.

Acknowledgements: The authors acknowledge support by the Open Access Publication Funds of Technische Universität Braunschweig. Part of Figure 8 was created with BioRender.com (under license number 307CB98D-0001 BioRender). The IMPACT operation has been partfunded by the European Regional Development Fund through the Welsh Government (c80843) and Swansea University.

Funding information: The authors gratefully acknowledge financial support from the German Research Foundation (DFG).

Author contributions: All authors have accepted responsibility for the entire content of this manuscript and approved its submission.

Conflict of interest: The authors state no conflict of interest.

References

- Li R, Pei J, Sun C. Effect of nano-ZnO with modified surface on properties of bitumen. Constr Build Mater. 2015;98:656-61.
- Sadeghnejad M, Shafabakhsh G. Experimental study on the physical and rheological properties of bitumen modified with different nano materials (Nano SiO₂ & Nano TiO₂). Int J Nano Nanotech. 2017;13(3):253-63.
- Shafabakhsh G, Ani OJ. Experimental investigation of effect of Nano TiO₂/SiO₂ modified bitumen on the rutting and fatigue performance of asphalt mixtures containing steel slag aggregates. Constr Build Mater. 2015;98:692-702.
- Sun X, Yuan J, Zhang Y, Yin Y, Lv J, Jiang S. Thermal aging behavior characteristics of asphalt binder modified by nano-

- stabilizer based on DSR and AFM. Nanotech Rev. 2021:10(1):1157-82.
- [5] Li Z, Guo T, Chen Y, Liu Q, Chen Y. The properties of nano-CaCO₃/nano-ZnO/SBR composite-modified asphalt. Nanotech Rev. 2021;10(1):1253-65.
- Rad FY, Elwardany MD, Castorena C, Kim YR. Evaluation of chemical and rheological aging indices to track oxidative aging of asphalt mixtures. Tran Res Rec. 2018;2672(28):349-58.
- Zhu C, Xu G, Zhang H, Xiao F, Amirkhanian S, Wu C. Influence of different anti-stripping agents on the rheological properties of asphalt binder at high temperature. Constr Build Mater. 2018;164:317-25.
- Cheraghian G, Wistuba MP. Ultraviolet aging study on bitumen modified by a composite of clay and fumed silica nanoparticles. Sci Rep. 2020;10(1):11216.
- Lin M, Wang ZL, Yang PW, Li P. Micro-structure and rheological properties of graphene oxide rubber asphalt. Nanotech Rev. 2019;8(1):227-35.
- [10] Cheraghian G, wang D, Kim Y, Wistuba M, editors. Experimental investigation on ultraviolet aging properties of silica nanoparticles-modified bitumen. RILEM ISBM Lyon 2020. Lyon, France: RILEM, Springer; 2020.
- [11] Kleizienė R, Paliukaitė M, Vaitkus A, editors. Effect of nano SiO₂, TiO₂ and ZnO modification to rheological properties of neat and polymer modified bitumen. International Symposium on Asphalt Pavement & Environment. Springer; 2019.
- [12] Cheraghian G. Evaluation of clay and fumed silica nanoparticles on adsorption of surfactant polymer during enhanced oil recovery. J Jpn Pet Ins. 2017;60(2):85-94.
- [13] Cheraghian G, Falchetto AC, You Z, Chen S, Kim YS, Westerhoff J, et al. Warm mix asphalt technology: an up to date review. J Clean Prod. 2020;268:122128.
- [14] Ahmad N, Nasir MA, Hafeez M, Rafi J, Zaidi SBA, Haroon W. Carbon nanotubes (CNTs) in asphalt binder: homogeneous dispersion and performance enhancement. App Sci. 2018;8(12):2651.
- [15] Amin GM, Esmail A. Application of nano silica to improve selfhealing of asphalt mixes. J Cent S Uni. 2017;24(5):1019-26.
- [16] Cheraghian G, Wistuba MP. Effect of Fumed silica nanoparticles on ultraviolet aging resistance of bitumen. Nanomaterials. 2021 Feb;11(2):454.
- [17] Azarhoosh A, Moghaddas Nejad F, Khodaii A. Evaluation of the effect of nano-TiO2 on the adhesion between aggregate and asphalt binder in hot mix asphalt. Eur J Envoi Civ Eng. 2018;22(8):946-61.
- [18] Cheraghian G, Wistuba MP, Kiani S, Barron AR, Behnood A. Rheological, physicochemical, and microstructural properties of asphalt binder modified by fumed silica nanoparticles. Sci Rep. 2021;11(1):1-20.
- Enieb M, Diab A. Characteristics of asphalt binder and mixture containing nanosilica. Int J Pav Res Tech. 2017;10(2):148-57.
- Cheraghian G. Synthesis and properties of polyacrylamide by [20] nanoparticles, effect nanoclay on stability polyacrylamide solution. Micro Nano Lett. 2017;12(1):40-4.
- [21] Ceccon Carlesso G, Trichês G, Staub de Melo JV, Marcon MF, Padilha Thives L, da Luz LCJAS. Evaluation of rheological behavior, resistance to permanent deformation, and resistance to fatigue of asphalt mixtures modified with nanoclay and SBS polymer. Appl Sci. 2019;9(13):2697.

- [22] Qian G, Yang C, Huang H, Gong X, Yu H. Resistance to ultraviolet aging of nano-sio2 and rubber powder compound modified asphalt. Materials. 2020;13(22):5067.
- [23] Cheraghian G. Application of nano-particles of clay to improve drilling fluid. int j of nanoscience. Nanotechnology. 2017;13(2):177-86.
- [24] Ranjbarzadeh R, Moradikazerouni A, Bakhtiari R, Asadi A, Afrand M. An experimental study on stability and thermal conductivity of water/silica nanofluid: eco-friendly production of nanoparticles. J Clean Prod. 2019;206:1089-100.
- [25] Guo C, Jordan JS, Yarger JL, Holland GP. Highly Efficient fumed silica nanoparticles for peptide bond formation: converting alanine to alanine anhydride. ACS App Mater Interfaces. 2017:9(20):17653-61.
- [26] Behnood A, Karimi MM, Cheraghian G. Coupled effects of warm mix asphalt (WMA) additives and rheological modifiers on the properties of asphalt binders. Clean Eng Tech. 2020;1:100028.
- [27] Fakhri M, Javadi S, Sedghi R, Arzjani D, Zarrinpour Y. Effects of deicing agents on moisture susceptibility of the WMA containing recycled crumb rubber. Constr Build Mater. 2019;227:116581.
- [28] Ameri M, Yazdipanah F, Rahimi Yengejeh A, Afshin A. Production temperatures and mechanical performance of rubberized asphalt mixtures modified with two warm mix asphalt (WMA) additives. Mater Struct. 2020;53(4):113.
- [29] Cheraghian G, Wu Q, Mostofi M, Li M-C, Afrand M, Sangwai JS. . Effect of a novel clay/silica nanocomposite on water-based drilling fluids: improvements in rheological and filtration properties. Colloids Surf A: Physicochem Eng Asp. 2018;555:339-50.
- [30] Gwyddion.net. Gwyddion Download. [Online]. http:// gwyddion.net/download.php. 2020.
- [31] Omar HA, Yusoff NIM, Ceylan H, Rahman IA, Sajuri Z, Jakarni FM, et al. Determining the water damage resistance of nano-clay modified bitumens using the indirect tensile strength and surface free energy methods. Constr Build Mater. 2018:167:391-402.
- [32] Tseng T-F, Wu J-Y. Preparation and structural characterization of novel nanohybrids by cationic 3D silica nanoparticles sandwiched between 2D anionic montmorillonite clay through electrostatic attraction. J Phy Chemi C. 2009;113(30):13036-44.
- [33] Nivedya MK, Trottier TG, Yu X, Tao M, Burnham NA, Mallick RB. Microstructural evolution of asphalt binder under combined action of moisture and pressure. J Trans Eng Part B: Pavements. 2019;145(2):06019001.
- [34] Soenen H, Besamusca J, Fischer HR, Poulikakos LD, Planche J-P, Das PK, et al. Laboratory investigation of bitumen based on round robin DSC and AFM tests. Mater Struct. 2014;47(7):1205-20.
- [35] Hofko B, Eberhardsteiner L, Füssl J, Grothe H, Handle F, Hospodka M, et al. Impact of maltene and asphaltene fraction on mechanical behavior and microstructure of bitumen. Mater Struct. 2016;49(3):829-41.
- [36] Nazzal Munir D, Abu-Qtaish L, Kaya S, Powers D. Using atomic force microscopy to evaluate the nanostructure and nanomechanics of warm mix asphalt. J Mater Civ Eng. 2015;27(10):04015005.
- [37] Zhang H, Wang Y, Yu T, Liu Z. Microstructural characteristics of differently aged asphalt samples based on atomic force microscopy (AFM). Const Build Mater. 2020;255:119388.

- [38] Anderson DA, Christensen DW, Bahia HU, Dongre R, Sharma M, Antle CE, et al. Binder characterization and evaluation. Phys Charact. 1994;3:491.
- [39] Cao Z, Chen M, He B, Han X, Yu J, Xue L. Investigation of ultraviolet aging resistance of bitumen modified by layered double hydroxides with different particle sizes. Const Build Mater. 2019;196:166-74.
- [40] Molenaar AAA, Hagos ET, van de Ven MFC. Effects of aging on the mechanical characteristics of bituminous binders in PAC. J Mater Civ Eng. 2010;22(8):779-87.
- [41] Nciri N, Kim J, Kim N, Cho N. An in-depth investigation into the physicochemical, thermal, microstructural, and rheological properties of petroleum and natural asphalts. Materials. 2016:9(10):859.
- [42] Li Y-B, Luo C, Lin X, Li K, Xiao Z-R, Wang Z-Q, et al. Characteristics and properties of coke formed by low-temperature oxidation and thermal pyrolysis during in situ combustion. I&EC. 2020;59(5):2171-80.
- [43] Khairuddin FH, Alamawi MY, Yusoff NIM, Badri KH, Ceylan H, Tawil SNM. Physicochemical and thermal analyses of polyurethane modified bitumen incorporated with Cecabase and Rediset: optimization using response surface methodology. Fuel. 2019;254:115662.
- [44] Liu W, Miao P, Wang S-Y. Increasing microwave heating efficiency of asphalt-coated aggregates mixed with modified steel slag particles. J Mater Civ Eng. 2017;29(10):04017171.
- [45] Li C, Wu S, Chen Z, Tao G, Xiao Y. Improved microwave heating and healing properties of bitumen by using nanometer microwave-absorbers. Constr Build Mater. 2018;189:757-67.
- [46] Kie Badroodi S, Reza Keymanesh M, Shafabakhsh G. Experimental investigation of the fatigue phenomenon in nano silica-modified warm mix asphalt containing recycled asphalt considering self-healing behavior. Constr Build Mater. 2020;246:117558.
- [47] Zhang Z, Cheng P, Li Y. Effect of nano montmorillonite on the multiple self-healing of microcracks in asphalt mixture. Road Mater Pave Des. 2020;12:1-15.
- [48] Fang C, Yu X, Yu R, Liu P, Qiao X. Preparation and properties of isocyanate and nano particles composite modified asphalt. Const Build Mater. 2016;119:113-8.
- [49] Xu X, Guo H, Wang X, Zhang M, Wang Z, Yang B. Physical properties and anti-aging characteristics of asphalt modified with nano-zinc oxide powder. Constr Build Mater. 2019;224:732-42.
- [50] Qing Z, Qi-Cheng L, Peng L, Chuan-Sheng C, Jiang-Rong K. Study on modification mechanism of nano-ZnO/polymerised styrene butadiene composite-modified asphalt using density functional theory. Road Mater Pave Des. 2020;21(5):1426-38.
- [51] Soleymanzadeh A, Yousefi M, Kord S, Mohammadzadeh O. A review on methods of determining onset of asphaltene precipitation. J Petr Exp Prod Tech. 2019;9(2):1375-96.
- [52] Galooyak SS, Dabir B, Nazarbeygi AE, Moeini A. Rheological properties and storage stability of bitumen/SBS/montmorillonite composites. Const Build Mater. 2010;24(3):300-7.
- [53] Zhu J, Birgisson B, Kringos N. Polymer modification of bitumen: advances and challenges. Euro Poly J. 2014;54:18-38.
- [54] Yao H, You Z, Li L, Lee Chee H, Wingard D, Yap Yoke K, et al. Rheological properties and chemical bonding of asphalt

- modified with nanosilica. J Mater Civ Eng. 2013;25(11):1619-30.
- [55] Liu K, Zhang K, Wu J, Muhunthan B, Shi X. Evaluation of mechanical performance and modification mechanism of asphalt modified with graphene oxide and warm mix additives. J Clean Prod. 2018;193:87-96.
- [56] Xue C-H, Zhao L-L, Guo X-J, Ji Z-Y, Wu Y, Jia S-T, et al. Mechanically durable superhydrophobic surfaces by binding polystyene nanoparticles on fibers with aluminum phosphate followed by hydrophobization. Chem Eng J. 2020;396:125231.
- [57] Huang X-J, Zeng X-F, Wang J-X, Zhang L-L, Chen J-F. Synthesis of monodispersed ZnO@SiO2 nanoparticles for anti-UV aging application in highly transparent polymer-based nanocomposites. J Mater Sci. 2019;54(11):8581-90.
- [58] Kiani S, Jones DR, Alexander S, Barron AR. New insights into the interactions between asphaltene and a low surface energy anionic surfactant under low and high brine salinity. J Coll Inter Sci. 2020;571:307-17.

- [59] Alabi O, Edilbi A, Brolly C, Muirhead D, Parnell J, Stacey R, et al. Asphaltene detection using surface enhanced Raman scattering (SERS). Chem Comm. 2015;51(33):7152-5.
- [60] Beyssac O, Goffé B, Chopin C, Rouzaud JN. Raman spectra of carbonaceous material in metasediments: a new geothermometer. J Meta Geo. 2002;20(9):859-71.
- [61] Katagiri G, Ishida H, Ishitani A. Raman spectra of graphite edge planes. Carbon. 1988;26(4):565-71.
- [62] Mortezaei M, Shabani S, Mohammadian-Gerzaz S. Assessing the effects of premixing on the rheological properties for three-phases asphalt binder nano-composite including clay and SBS. Const Build Mater. 2020;231:117151.
- [63] Nejad FM, Nazari H, Naderi K, Karimiyan Khosroshahi F, Hatefi, Oskuei M. Thermal and rheological properties of nanoparticle modified asphalt binder at low and intermediate temperature range. Petro Sci Tech. 2017;35(7):641-6.
- [64] Farahani H, Palassi M, Galooyak S. Rheology investigation of waste LDPE and crumb rubber modified bitumen. Eng Solid Mech. 2018;6(1):27-38.